

Probing the Molecular Interaction of Triazole Fungicides with Human Serum Albumin by Multispectroscopic Techniques and Molecular Modeling

Jing Zhang, Shulin Zhuang,* Changlun Tong, and Weiping Liu*

College of Environmental and Resource Sciences, Zhejiang University, Hangzhou 310058, China

S Supporting Information

ABSTRACT: Triazole fungicides, one category of broad-spectrum fungicides, are widely applied in agriculture and medicine. The extensive use leads to many residues and casts potential detrimental effects on aquatic ecosystems and human health. After exposure of the human body, triazole fungicides may penetrate into the bloodstream and interact with plasma proteins. Whether they could have an impact on the structure and function of proteins is still poorly understood. By using multispectroscopic techniques and molecular modeling, the interaction of several typical triazole fungicides with human serum albumin (HSA), the major plasma protein, was investigated. The steady-state and time-resolved fluorescence spectra manifested that static type, due to complex formation, was the dominant mechanism for fluorescence quenching. Structurally related binding modes speculated by thermodynamic parameters agreed with the prediction of molecular modeling. For triadimefon, hydrogen bonding with Arg-218 and Arg-222 played an important role, whereas for imazalil, myclobutanil, and penconazole, the binding process was mainly contributed by hydrophobic and electrostatic interactions. Via alterations in three-dimensional fluorescence and circular dichroism spectral properties, it was concluded that triazoles could induce slight conformational and some microenvironmental changes of HSA. It is anticipated that these data can provide some information for possible toxicity risk of triazole fungicides to human health and be helpful in reinforcing the supervision of food safety.

KEYWORDS: triazole fungicides, human serum albumin, fluorescence spectroscopy, circular dichroism, molecular modeling

■ INTRODUCTION

Triazole fungicides are applied as agrichemicals to prevent fungal growth on fruits, vegetables, cereals, and seeds and on residential and commercial turf as well as in pharmaceutical applications for the treatment of topical and systemic fungal infections.^{1,2} The widespread use of triazoles has generated extensive concerns regarding their possible exposure to and detrimental effects on aquatic ecosystems³ and human health. Some members of this class have been observed to be hepatotoxic,^{3,4} tumorigenic,⁵ endocrine disrupting,² and able to affect gene expression⁶ in a series of toxicological studies. Recently, many triazole fungicides (e.g., triadimefon, imazalil, myclobutanil, propiconazole) have been found in excess residues in agricultural products such as tea, beverages, litchi, cabbage, and pea. After exposure to these substances, potential biological toxicity risks to the human body exist. It is known that the distribution, free concentration, and metabolism of various small molecules are affected by the ligand–protein interactions in the bloodstream.⁷ When these fungicides penetrate into the bloodstream, they may bind to plasma proteins and subsequently induce some alterations of the protein structure and function. As yet, only a few studies have been carried out to examine the toxic effects of triazoles at the protein level,⁸ and information about the possible impact on plasma proteins is still limited. Food safety remains a public issue all over the world, and thus some efforts should be taken to fill the data gap.

Human serum albumin (HSA) is the principal extracellular protein most abundant in blood plasma, corresponding to a

concentration of 42 mg/mL.⁹ It exhibits several crucial physiological and pharmacological functions, maintaining osmotic blood pressure, buffering pH, and serving in the transportation and distribution of a variety of substances such as fatty acids, amino acids, hormones, and pharmaceuticals. HSA is a heart-shaped globular protein comprising 585 amino acid residues in a single polypeptide chain stabilized by 17 disulfide bridges. It consists of three homologous domains (I–III), each of which can be divided into two subdomains (A and B).^{10,11} Two high-affinity binding sites, namely Sudlow's sites I and II, are located within specialized hydrophobic cavities in subdomains IIA and IIIA, respectively. The single tryptophan residue in HSA is Trp-214 in the subdomain IIA (site I),¹² which offers an advantage to study the ligand binding process by intrinsic fluorescence.

Spectroscopic techniques have become popular methods for revealing protein–ligand interactions and structural characterization of proteins because of their high sensitivity, rapidity, reproducibility, and convenience.⁷ They allow nondestructive measurements of substances in low concentration under physiological conditions.⁸ The objective of the present work was to explore the interaction mechanism of typical triazole fungicides with HSA. Multispectroscopic approaches were adopted to determine the binding properties and the effects

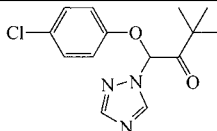
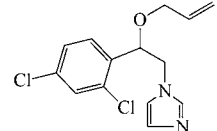
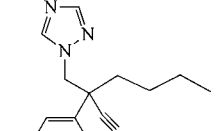
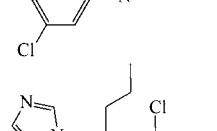
Received: March 12, 2013

Revised: July 6, 2013

Accepted: July 8, 2013

Published: July 8, 2013

Table 1. Chemical Structures of Four Triazole Fungicides

Triazole Fungicides	CAS Number	Chemical Structure
triadimefon	43121-43-3	
imazalil	35554-44-0	
myclobutanil	88671-89-0	
penconazole	66246-88-6	

of complexation on the protein structure and to characterize the main acting forces. Our results showed that certain triazoles significantly caused the fluorescence quenching of HSA and aroused conformational and microenvironmental changes of the protein. The binding mode was further elucidated by molecular docking at the atomic level. These results may provide basic data for clarifying the binding mechanisms of triazoles with HSA and be helpful for food security and human health when triazole is applied as an antifungal agent.

MATERIALS AND METHODS

Chemicals and Reagents. All of the tested triazole fungicides (Table 1 and Table S5 of the Supporting Information) with purity >96% were purchased from Dr. Ehrenstorfer Co. (Germany). The stock solutions were prepared in absolute ethanol. Human serum albumin (purity = 96–99%) was purchased from Sigma-Solarbio Co. (Beijing, China) and was used without further purification. HSA solution (1.5 μM) was prepared in Tris-HCl buffer (0.2 M Tris, 0.1 M NaCl, pH 7.40) and conserved in the dark at 4 °C. Phosphate buffer (0.02 M, pH 7.40) was used in circular dichroism measurements to avoid the influence of chloride ions. Other chemicals and reagents used in this study were all of analytical grade. Milli-Q water (18.2 M Ω , Millipore, Bedford, MA, USA) was used throughout the experiments.

Fluorescence Measurements. Fluorescence spectra measurements were performed on an F-2500 spectrofluorophotometer (Hitachi, Japan) equipped with a 1.0 cm quartz cell and a thermostat bath. A 3 mL solution containing HSA with the fixed concentration of 1.5 μM was titrated by successive additions of triazole fungicides (experimental concentration varied from 3.0 to 30.0 μM). The excitation wavelength was set at 280 nm, and the emission was recorded from 300 to 500 nm. All experiments were measured at three different temperatures (296, 303, and 310 K).

Synchronous fluorescence spectra were made on the F-2500 spectrofluorometer at room temperature. The scanning interval between excitation and emission wavelength ($\Delta\lambda$) was stabilized at 15 and 60 nm, respectively, and the emission was recorded in the range of 250–350 nm.

To evaluate existing inner filter effects, absorbance measurements were performed at excitation and emission wavelengths of albumin. Observed fluorescence values were corrected by the equation¹³

$$F_{\text{cor}} = F_{\text{obs}} e^{(A_{280} + A_{334})/2} \quad (1)$$

where F_{cor} and F_{obs} represent the corrected and observed fluorescence intensities and A_{280} and A_{334} are the sums of the absorbance of protein and ligand at the excitation and emission wavelengths, respectively.

Fluorescence lifetimes were measured from time-resolved intensity decay by time correlated single-photon counting (TCSPC) method, using a Jobin-Yvon FluoroMax-4 spectrometer (Horiba, Japan). A picosecond diode laser (NanoLED-280) as the light source at 280 nm was applied to selectively excite HSA, and the emission was monitored at 334 nm. The fluorescence decay was acquired with 1024 channels and a peak preset of 10000 counts. DAS6 software was used to deconvolute the fluorescence decays and calculate the lifetimes.

Three-dimensional fluorescence spectra were obtained on the Jobin-Yvon FluoroMax-4 spectrometer. The initial excitation wavelength was set at 200 nm with increments of 4 nm, and the emission wavelength was recorded from 200 to 500 nm with increments of 2 nm. The scan rate was set to 200 nm min⁻¹.

Circular Dichroism (CD) Studies. CD measurements were performed on a Jasco J-815 CD spectrometer (Japan Spectroscopic, Japan) in a 1.0 cm path length cell at room temperature under constant nitrogen flush. The spectra of HSA in the presence of triazole fungicides were recorded in the range of 200–260 nm with a scan rate of 50 nm min⁻¹. Three scans were accumulated for each spectrum, taking the average as the final data. The HSA secondary structure based on CD data was computed using Jasco Secondary Structure Estimation (SSE) software.

Molecular Docking. The crystal structure of HSA in complex with *R*-warfarin (entry code 1H9Z, Brookhaven Protein Data Bank)¹⁴ was chosen as the template. The protein structure was carefully checked for atom and bond type correctness assignment. All solvent molecules and ligands were removed, and explicit hydrogen atoms were computationally added at appropriate geometry; this procedure did not change positions of heavy atoms.¹⁵ The triazole fungicides were automatically docked into HSA using Gold suite 5.0.¹⁶ Fifty genetic algorithm (GA) runs were performed to search the binding conformations of each

ligand with default parameters. The binding energies were scored by GoldScore and rescored by CHEMPLP, respectively. On the basis of the scores and visual inspection, the most possible poses were selected for structural analysis.

RESULTS AND DISCUSSION

Fluorescence Quenching of HSA upon Addition of Triazole Fungicides. Fluorescence spectroscopy is an effective method to study the interactions between small molecule ligands and biomacromolecules. The representative spectra of HSA in the absence and presence of triazole fungicides are shown in Figure 1 and Figures S1 and S2 of the

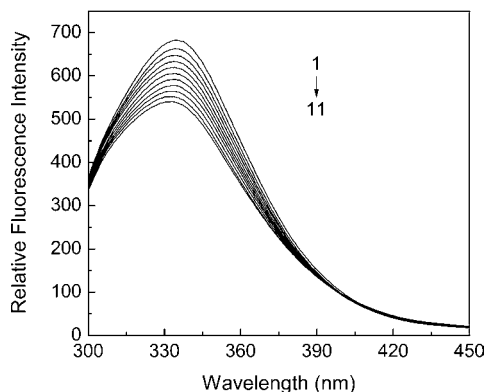


Figure 1. Effect of myclobutanil on the fluorescence spectra of HSA. $c(\text{HSA}) = 1.5 \mu\text{M}$. Lines 1–11: $c(\text{myclobutanil}) = 0, 3.0, 6.0, 9.0, 12.0, 15.0, 18.0, 21.0, 24.0, 27.0, 30.0 \mu\text{M}$, respectively; $\lambda_{\text{ex}} = 280 \text{ nm}$; $\lambda_{\text{em}} = 334 \text{ nm}$; $\text{pH} = 7.40$; $T = 296 \text{ K}$.

Supporting Information. It can be seen that the fluorescence intensity of HSA decreases regularly with the increasing concentration of triazoles, which is called the fluorescence quenching effect. The maximum emission wavelength of HSA is almost unchanged, suggesting the small molecules are likely to interact with HSA via a hydrophobic region located inside the protein.¹⁷ Triadimefon, imazalil, myclobutanil, and penconazole (Table 1) displayed distinct quenching phenomenon among the eight tested fungicides and thus were chosen for further analysis.

A variety of molecular interactions can induce fluorescence quenching, including ground state complex formation, excited state reactions, energy transfers, and collisional processes among others. Generally, the quenching mechanisms are classified into dynamic quenching and static quenching, which can be distinguished by their different dependences on temperature and viscosity or preferably by lifetime measurements.⁷ Dynamic quenching mainly depends on diffusion, so quenching constants of the fluorescent complexes are expected to increase with a rise in temperature, and the maximum scatter collision quenching constant of the biomolecule by all kinds of quenchers (limiting diffusion constant, K_{diff}) is $2.0 \times 10^{10} \text{ L mol}^{-1} \text{ s}^{-1}$.^{13,18} On the contrary, the increase of temperature is likely to result in decreased stability of complexes; thus, values of static quenching constants will be lower.¹⁹

The possible quenching mechanism can be described by the Stern–Volmer equation^{20,21}

$$F_0/F = 1 + K_q\tau_0[Q] = 1 + K_{\text{SV}}[Q] \quad (2)$$

where F_0 and F are the fluorescence intensities of protein in the absence and presence of quencher, respectively. K_q is the

quenching rate constant of the biomolecule, τ_0 is the average lifetime of the biomolecule without quencher (about 10 ns for most biomolecules),²² $[Q]$ is the concentration of quencher, and K_{SV} is the Stern–Volmer constant.

The curves of F_0/F versus $[Q]$ at three different temperatures are presented in Figure 2 (e.g., myclobutanil), and the

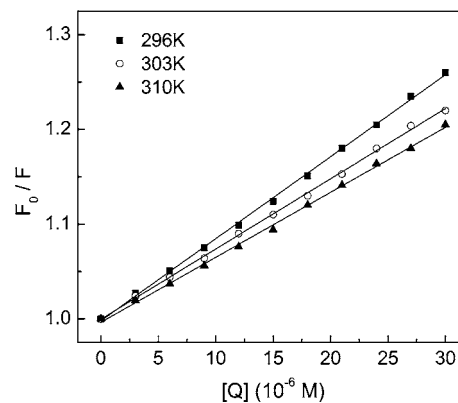


Figure 2. Stern–Volmer plots for fluorescence quenching of the HSA–myclobutanil system at different temperatures. $c(\text{HSA}) = 1.5 \mu\text{M}$; $c(\text{myclobutanil}) = 0–30.0 \mu\text{M}$; $\lambda_{\text{ex}} = 280 \text{ nm}$; $\lambda_{\text{em}} = 334 \text{ nm}$; $\text{pH} = 7.40$; $T = 296, 303, \text{ and } 310 \text{ K}$.

corresponding K_q and K_{SV} are summarized in Table S1 of the Supporting Information. The K_q value is much greater than K_{diff} , and the K_{SV} value is inversely correlated with the temperature, implying that the quenching mechanism of HSA by triazole fungicides is not initiated by dynamic collision but proceeds from static quenching.

Identification of Binding Parameters. On the basis of the above conclusion, the association constant (K_A) and the number of binding sites (n) can be calculated by the Lineweaver–Burk equation¹³ and Scatchard equation

$$\frac{1}{F_0 - F} = \frac{1}{F_0} + \frac{K_D}{F_0[Q]} \quad (3)$$

where K_D is the dissociation constant and F_0 , F , and $[Q]$ represent the same quantities as given for eq 1.

The Lineweaver–Burk double-reciprocal plot is constructed by the relationship of $1/(F_0 - F)$ versus $1/[Q]$ (Figure S3-A of the Supporting Information, e.g., myclobutanil), and from the linear regression equation of curves, association constants ($K_A = 1/K_D$) can be obtained (Table S2 of the Supporting Information).

The Scatchard equation is used to estimate the number of binding sites involved in the binding interaction; it is described as^{11,13}

$$\log\left(\frac{F_0 - F}{F}\right) = \log K_A + n \log[Q] \quad (4)$$

where K_A represents the association constant, n is the number of binding sites, and the meanings of F_0 , F , and $[Q]$ are the same as for eq 1.

Figure S3-B of the Supporting Information displays the plots of $\log(F_0 - F)/F$ versus $\log[Q]$ for the interaction between HSA and triazole fungicides (e.g., myclobutanil) at various temperatures. K_A and n obtained from the plots are listed in Table S3 of the Supporting Information.

Table 2. Association Constants (by Lineweaver–Burk Equation) and Thermodynamic Parameters for the Interaction between Triazole Fungicides and HSA

	<i>T</i> (K)	<i>K_A</i> (L mol ⁻¹)	Δ <i>G</i> (kJ mol ⁻¹)	Δ <i>H</i> (kJ mol ⁻¹)	Δ <i>S</i> (J mol ⁻¹ K ⁻¹)
triadimefon	296	3.96 × 10 ³	-20.38	-43.27	-77.13
	303	2.81 × 10 ³	-20.01		
	310	1.79 × 10 ³	-19.30		
imazalil	296	8.62 × 10 ³	-22.30	-19.55	9.29
	303	7.14 × 10 ³	-22.35		
	310	6.02 × 10 ³	-22.43		
myclobutanil	296	8.79 × 10 ³	-22.35	-13.28	30.71
	303	7.97 × 10 ³	-22.63		
	310	6.90 × 10 ³	-22.78		
penconazole	296	8.47 × 10 ³	-22.26	-14.24	27.14
	303	7.52 × 10 ³	-22.48		
	310	6.54 × 10 ³	-22.64		

The results show that the association constants calculated by both equations are in good agreement. The trend of decreasing *K_A* values with increasing temperature is similar to that observed with the *K_{SV}* values, thus further supporting static quenching as the dominant mechanism for the HSA–triazole fungicide systems. The number of binding sites in HSA approximates to 1, indicating that only one site is reactive to triazole fungicides in the experimental concentration range.

Thermodynamic Parameters and Acting Forces. The interaction forces between small molecules and biomolecules mainly include four types: hydrogen bonding; hydrophobic interaction; ionic, electrostatic interaction; and van der Waals force. The thermodynamic parameters, free energy change (Δ*G*), enthalpy change (Δ*H*), and entropy change (Δ*S*) of the binding reaction can provide evidence for clarifying interaction modes. If Δ*H* does not change significantly over the temperature range studied, it can be regarded as a constant, and then the values of Δ*H*, Δ*S*, and Δ*G* are estimated from the van't Hoff equation

$$\ln K_A = -\Delta H/RT + \Delta S/R \quad (5)$$

$$\Delta G = \Delta H - T\Delta S \quad (6)$$

where *K_A* is the association constant at temperature *T* and *R* is the universal gas constant.

Nemethy and Scheraga²³ and Ross and Subramanian^{24,25} have characterized the signs and magnitudes of the thermodynamic parameters associated with various individual kinds of interaction that might take place in the protein association processes. That is, for Δ*H* > 0 and Δ*S* > 0, the contributions to these changes mainly arise from hydrophobic interactions; for Δ*H* < 0 and Δ*S* < 0, van der Waals forces and hydrogen bond formation play major roles, whereas for Δ*H* ≈ 0 and Δ*S* > 0, electrostatic forces are suggested as more important.²⁶

The calculated Δ*H*, Δ*S*, and Δ*G* are summarized in Table 2. The Δ*G* value is negative, indicating that the binding process is spontaneous. For triadimefon, the values of both Δ*H* and Δ*S* were negative, which suggested the main acting force would be hydrogen bonding and/or van der Waals force. It seems understandable when considering the chemical structure. The carbonyl group is a neutral acceptor group for hydrogen bonding; the ether link in the main chain might show some different properties compared to the other three and can also

potentially form a hydrogen bond. For imazalil, myclobutanil, and penconazole, Δ*S* values were found to be positive, whereas Δ*H* values were negative. Binding of the ligand to the protein would lead to the burial of solvent-accessible surface or solvent release from the surface; thus, the system undergoes a favorable entropic change. In this view, the positive Δ*S* values are supposed to provide evidence for hydrophobic interactions in the binding phenomenon between HSA and these three fungicides, whereas the electrostatic interaction could not be excluded. Meanwhile, the negative Δ*H* values may account for the involvement of hydrogen bonding in this interaction, as N atoms on the triazole ring can easily form hydrogen bonds with amino acid residues such as arginine (Arg). As to imazalil particularly, both the Δ*S* and Δ*H* values are lower, perhaps implying that the binding process is predominately enthalpy driven, and hydrophobic interaction would be relatively weaker. This can also be explained by the differences in chemical structure; imazalil has only two N atoms in the triazole ring, and the ether link in the side chain may influence its lipophilicity, electrostatic potential, and contacts with surrounding amino acid residues. Besides, triazoles contain aromatic rings; therefore, π–π stacking with amino acid residues such as tryptophan (Trp), tyrosine (Tyr), and histidine (His) in HSA is also reasonable.

Synchronous Fluorescence Spectroscopy. The molecular environment in the vicinity of a fluorophore was studied by synchronous fluorescence spectroscopy. In this method, the sensitivity associated with fluorescence is maintained, whereas several advantages are offered, such as spectrum simplification, spectral bandwidth reduction, and avoiding different perturbing effects.¹³ When the wavelength differences (Δ*λ*) of excitation and emission were fixed at 15 and 60 nm, respectively, the spectrum would provide the characteristic information of tyrosine (Tyr) and tryptophan (Trp) residues in a protein, respectively.²⁷ The representative synchronous fluorescence spectra of HSA are shown in Figure 3. The maximum emission wavelengths of tyrosine and tryptophan residues remain unchanged during the interaction, suggesting that the polarity around these two residues is retained. However, compared with tyrosine residues, a stronger fluorescence quenching of tryptophan residues is observed on the addition of triazoles, which indicates that the binding site of triazoles is nearer tryptophan.

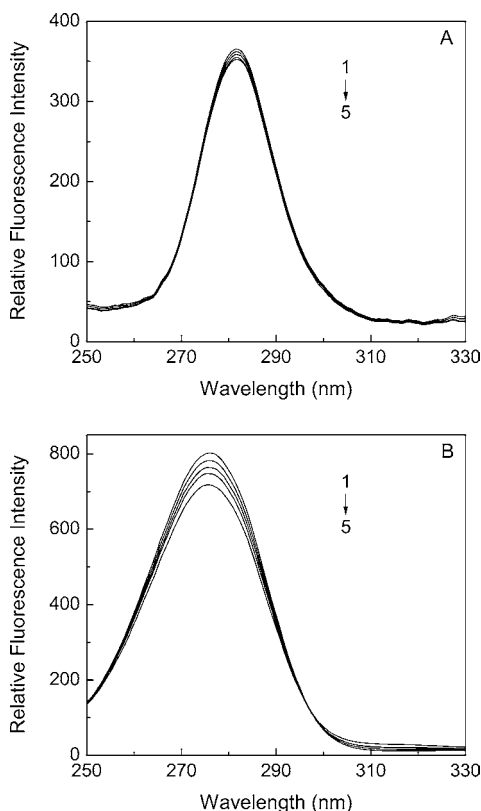


Figure 3. Effects of myclobutanil on the synchronous fluorescence spectra of HSA: (A) $\Delta\lambda = 15$ nm (tyrosine); (B) $\Delta\lambda = 60$ nm (tryptophan). $c(\text{HSA}) = 1.5 \mu\text{M}$. Lines 1–5: $c(\text{myclobutanil}) = 0, 7.5, 15.0, 22.5, 30.0 \mu\text{M}$, respectively; pH = 7.40; $T = 298$ K.

The result is in agreement with several reported experimental observations. The intrinsic fluorescence of HSA comes from three fluorophores, phenylalanine (Phe), tyrosine (Tyr), and tryptophan (Trp). Phenylalanine has a very low quantum yield, and the fluorescence of tyrosine is significantly quenched if it is ionized or near an amino group, a carboxyl group, or a tryptophan. Thus, a change in the intrinsic fluorescence intensity was mainly due to tryptophan residues when small molecules bound to HSA.²⁸ Trp-214 is the only tryptophan

residues in HSA and is buried deep in subdomain IIA, where a large hydrophobic cavity exists and small hydrophobic molecules can penetrate and bind. Therefore, it can be inferred that the primary binding site of triazole fungicides is likely to be subdomain IIA (site I), which prefers to accept bulky heterocyclic anions.^{9,29,30}

Fluorescence Lifetime Analysis. This approach is based on the fact that the fluorescence lifetime of tryptophan, the major endogenous fluorophore in albumin, is highly sensitive to the protein conformation. According to the theory of Lakowicz,²¹ fluorescence quenching process can be preferably distinguished by time-resolved fluorescence measurements immediately. The fluorescence decay patterns of HSA are shown in Figure S4 of the Supporting Information, and the calculated lifetimes and corresponding amplitudes are pooled in Table 3. The decay profiles are well fitted into a biexponential function, and the relative fluorescence lifetimes are $\tau_1 = 2.08$ ns and $\tau_2 = 6.41$ ns of HSA, whereas in the maximum concentration of triadimefon, imazalil, myclobutanil, and penconazole, the lifetimes are slightly increased to be $\tau_1 = 2.11/2.11/1.91/2.14$ ns and $\tau_2 = 6.45/6.35/6.51/6.34$ ns. Although HSA has only one tryptophan residue, it is known to display multiexponential decays. The heterogeneity of fluorescence lifetime has partly been ascribed to its local environment in the protein matrix, that is, the position of other amino acid residues adjacent to tryptophan.³¹ Obviously, the lifetimes and their amplitudes differed, which suggested that the tryptophan microenvironment might undergo some alteration. We have not tried to assign the individual components, and the average lifetime was chosen to acquire a qualitative analysis.^{15,32} The results show a negligible difference, indicating that fluorescence quenching caused by triazole fungicides in low concentrations is an essentially static mechanism. This observation coincides with the previous conclusions based on fluorescence spectroscopy and, additionally, these small molecules are likely to bind in the proximity of Trp-214 and arouse some microenvironmental changes.

Conformational Analysis of HSA after Triazole Binding. The binding of triazole fungicides to HSA induced fluorescence quenching; whether the secondary structure was affected remains unclear. Here, we utilized the methods of

Table 3. Fluorescence Lifetimes of HSA in the Absence and Presence of Triazole Fungicides

	$[Q_{\text{HSA}}]/[Q_{\text{TF}}]$	τ_1 (ns)	τ_2 (ns)	A_1	A_2	τ (ns)	χ^2
HSA		2.08	6.41	0.295	0.705	5.13	1.09
triadimefon	1:5	1.94	6.35	0.274	0.726	5.14	1.14
	1:10	1.96	6.37	0.282	0.718	5.13	1.19
	1:20	2.11	6.45	0.307	0.693	5.12	1.16
imazalil	1:5	2.05	6.27	0.272	0.728	5.12	1.13
	1:10	2.04	6.28	0.276	0.724	5.11	1.08
	1:20	2.11	6.35	0.291	0.709	5.12	1.22
myclobutanil	1:5	1.92	6.41	0.282	0.718	5.14	1.17
	1:10	1.85	6.36	0.275	0.725	5.12	1.15
	1:20	1.91	6.51	0.301	0.699	5.13	1.12
penconazole	1:5	1.99	6.27	0.267	0.733	5.13	1.17
	1:10	1.95	6.31	0.270	0.730	5.13	1.09
	1:20	2.14	6.34	0.285	0.715	5.14	1.14

three-dimensional (3D) fluorescence and CD spectroscopy to explore the conformational changes of HSA.

Three-Dimensional Fluorescence Spectroscopy. 3D fluorescence spectroscopy has been commonly applied for studying the interaction between small molecules and proteins in recent years. It can extensively reflect the fluorescence information of the protein, if there is a shift at the excitation or emission wavelength around the fluorescence peak, or the appearance of a new peak, or the disappearance of an existing one,²⁶ and all these pieces of evidence can help tell the characteristic conformational changes and make the investigation more scientific and credible.¹⁰ Figure 4 and Figure S5

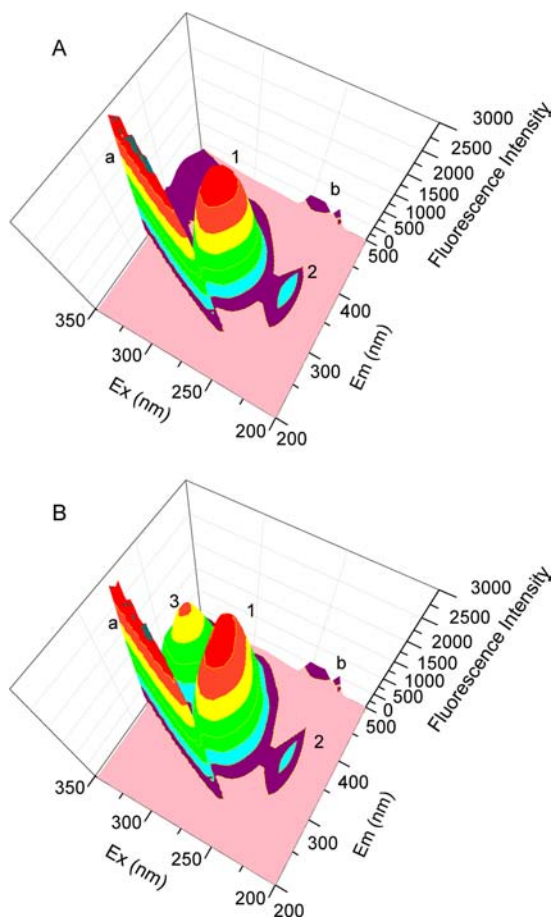


Figure 4. Three-dimensional fluorescence spectra of free HSA (A) and HSA in complex with myclobutanil (B). $c(\text{HSA}) = 1.5 \mu\text{M}$; $c(\text{myclobutanil}) = 30.0 \mu\text{M}$; pH = 7.40; $T = 298 \text{ K}$.

of the Supporting Information present the three-dimensional fluorescence spectra of free HSA and the HSA-triazole fungicide systems, and the corresponding parameters are collected in Table S4 of the Supporting Information. Peak a ($\lambda_{\text{ex}} = \lambda_{\text{em}}$) is the Rayleigh scattering peak, and peak b ($2\lambda_{\text{ex}} = \lambda_{\text{em}}$) is the second-order scattering peak, both common in all spectra. Peak 1 ($\lambda_{\text{ex}} = 280 \text{ nm}$, $\lambda_{\text{em}} = 334 \text{ nm}$) mainly exhibits the intrinsic fluorescence of Trp and Tyr residues involving $\pi \rightarrow \pi^*$ transition, reflecting the changes in the tertiary structure of HSA. Peak 2 ($\lambda_{\text{ex}} = 232 \text{ nm}$, $\lambda_{\text{em}} = 338 \text{ nm}$) relates to the fluorescence spectral behavior of polypeptide backbone structures and signifies the changes in the secondary structure of HSA.³³ Peak 3 represents the characteristic fluorescence of triazoles. From the figures, the fluorescence emission intensity

of peak 1 decreased upon the addition of triazole fungicides, revealing that the hydrophobic microenvironment near Trp and Tyr residues has been altered.¹⁷ Similarly, the fluorescence of peak 2 also turned out to be somewhat lower, which implied that binding of triazoles probably induced minor destabilization of HSA and a slight unfolding of the polypeptide backbone, resulting in conformational changes that increase the exposure of some hydrophobic regions that had been buried before.³⁴ All of these results indicate that these triazole fungicides have interacted with HSA and would lead to conformational and microenvironmental changes in the protein.

CD Response of HSA to Triazoles. Secondary structure is always associated with the biological activity of proteins. CD spectroscopy is a powerful and sensitive analytical technique used to investigate the various aspects of protein structure in aqueous solution and help better understand the interactions between protein and small molecules. As Figure 5 and Figure

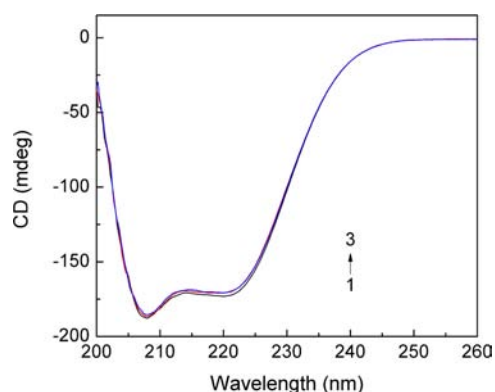


Figure 5. CD spectra of the HSA with increasing concentration of myclobutanil. $c(\text{HSA}) = 1.5 \mu\text{M}$; $c(\text{myclobutanil}) = 0, 7.5, 15.0 \mu\text{M}$; pH = 7.40; $T = 298 \text{ K}$.

S6 of the Supporting Information show, the CD curve of free HSA displays two negative bands in the far-UV region at 208 and 222 nm assignable to $\pi \rightarrow \pi^*$ and $n \rightarrow \pi^*$ transfers, which are typical of the α -helical structure of protein.³⁵ The ellipticity of HSA decreases slightly with the increase in concentration of triazoles, indicating some loss of α -helical content in HSA. The secondary structure components were calculated on the basis of raw CD data to quantitatively analyze the conformational changes. Free HSA has 51.7% α -helix, in the presence of triadimefon, imazalil, myclobutanil, and penconazole, the proportions lessen to 50.7, 49.9, 49.6, and 50.0%, respectively, at a molar ratio of 1:10. This may suggest that triazoles are able to interact with the amino acid residues of the polypeptide chain of HSA, partially destroy the hydrogen bonding networks,¹⁷ evoke some degree of protein destabilization,^{15,35} and adopt a more open conformation and better exposure of hydrophobic cavities.²⁶ Besides, the CD spectra before and after addition of triazoles are similar in shape, without any significant shift of the peaks, further confirming that α -helix is still the predominant conformation of HSA in this experimental system. All of the above analysis revealed that the binding of triazoles could cause slight conformational and some microenvironmental changes of HSA. Furthermore, the loss of α -helix partly resulted in better exposure of triazoles to hydrophobic regions, so it seems that hydrophobic interaction would play a more important role in stabilizing imazalil, myclobutanil, and

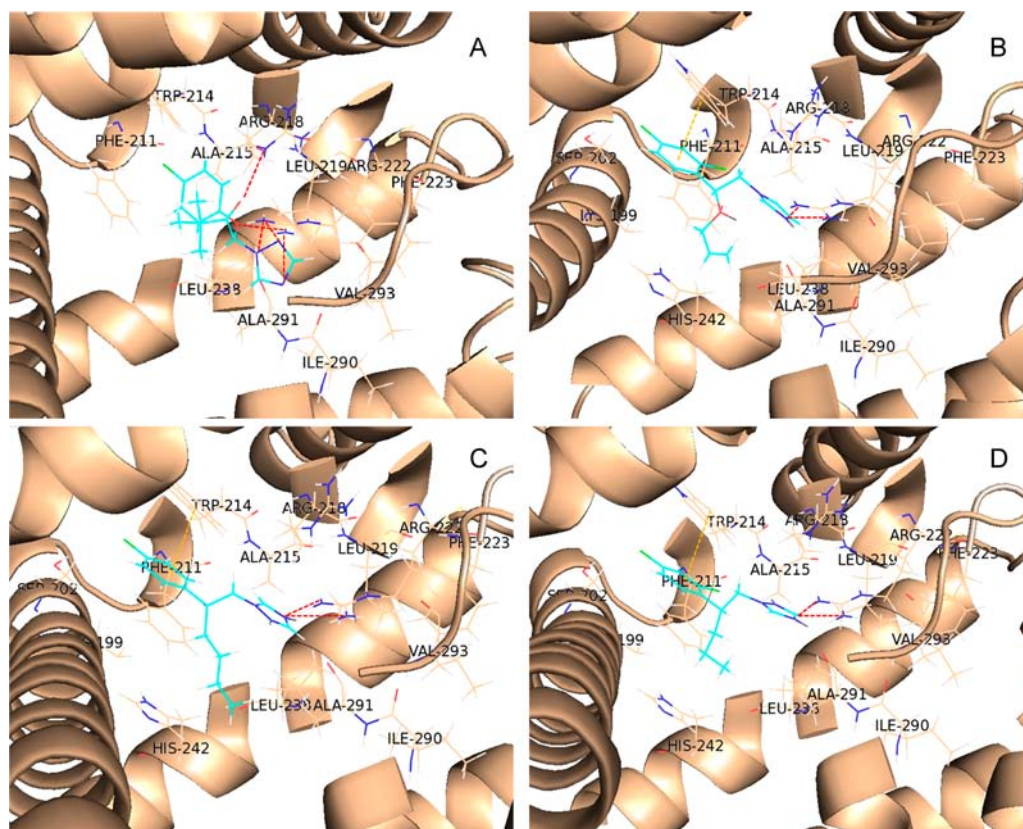


Figure 6. Binding modes of triadimefon (A), imazalil (B), myclobutanil (C), and penconazole (D) to HSA. The secondary structure of the protein is shown, and the important neighboring amino acid residues are labeled. The ligand structure is represented in a cyan stick format, hydrogen bond is indicated by a red dashed line, and π – π interaction by a yellow dashed line.

penconazole with HSA than triadimefon, which evidently coincides with the thermodynamic results.

Molecular Docking. The crystal structure of HSA complexed with *R*-warfarin was used as the initial template for molecular docking. The superimposition of the crystal and docked pose of *R*-warfarin gives a rmsd of 1.27 Å (Figure S7 of the Supporting Information), indicating that the applied docking procedure is reliable. Figure 6 and Figures S8 and S9 of the Supporting Information display the best binding modes of triazole fungicides to HSA and the lipophilicity and electrostatic potential of the ligand binding pocket in subdomain IIA (site I) of HSA, respectively.

All four of these fungicides were located deep in the hydrophobic cavity surrounded by the following amino acid residues: Lys-199, Ser-202, Phe-211, Trp-214, Ala-215, Arg-218, Leu-219, Arg-222, Phe-223, Leu-238, His-242, Ile-290, Ala-291, and Val-293. Log *P* (Table S5 of the Supporting Information) represents the lipophilicity of a compound. According to the fluorescence quenching results, generally a higher value of Log *P* always led to better binding affinity, supporting the importance of hydrophobic interactions to a certain extent, but the interaction cannot be presumed to be exclusively hydrophobic in nature, as there were several ionic as well as polar residues in the vicinity of the bound ligands, which would contribute to stabilizing the molecule via electrostatic interaction and hydrogen bonding, and the triazole ring was opposite a partially hydrophilic part. The electrostatic potential of the binding pocket was further investigated. It can be seen that it was almost positively charged, implying potential electrostatic interactions to certain electronegative atoms such

as O, N, and Cl. TopoPSA (Table S5 of the Supporting Information) features the electrostatic properties of a molecule, but there was no correlation, which means that TopoPSA did not show any capability to discriminate binding affinity in this experimental system. For triadimefon, five hydrogen bonds were predicted from the conformation as follows: the oxygen atom of the hydroxyl with Arg-218, the oxygen atom of the ether link, and the nitrogen atoms of the triazole ring with Arg-222. However, for imazalil, myclobutanil, and penconazole, the binding modes were quite alike: two hydrogen bonds were formed between each molecule and Arg-222 and, in addition, the aromatic ring displayed parallel π – π stacking with Trp-214.

The docking results agreed well with the thermodynamic analysis and illustrated that these triazole fungicides could interact with HSA in subdomain IIA (site I), similar to the previously reported propiconazole.⁸ Hydrophobic and electrostatic interactions are pervasive among the four fungicides with the protein. Hydrogen bonding plays a vital role in the binding process of triadimefon to HSA. Imazalil, myclobutanil, and penconazole share a similar binding mode. That is, hydrophobic interactions make a predominant contribution, hydrogen bonding and π – π stacking do exist, and the ether link in the branched chain of imazalil may influence its interaction to proximate amino acid residues to make the hydrophobic contacts comparably weaker. These conclusions provided a good structural basis to explain the fluorescence quenching phenomenon of HSA in the presence of triazole fungicides.

To sum up, the present study investigated the interaction of several typical triazole fungicides with HSA by multispectroscopic methods and molecular modeling. The four triazoles,

triadimefon, imazalil, myclobutanil, and penconazole, can interact with HSA in vitro under simulative physiological conditions. Fluorescence quenching of HSA by triazoles could be attributed to a static mechanism in the range of experimental concentration, and the calculated thermodynamic parameters offered evidence of structurally related binding modes, which were in accordance with the molecular docking results. Synchronous fluorescence suggested that the most probable binding site was subdomain IIA (site I) where Trp-214 was located, which was also predicted by computational modeling. Furthermore, binding of triazoles led to slight conformational and some microenvironmental changes of HSA via fluorescence lifetime measurements, 3D fluorescence, and CD. Knowledge of their binding to HSA, the major plasma protein, is beneficial to understand the effects on protein function and the mechanisms of interaction during transportation and deposition in blood. This may provide some information or potential data basis for clarifying the dynamics of toxicity of triazoles to human body and is thus valuable in reinforcing the supervision of food safety.

■ ASSOCIATED CONTENT

📄 Supporting Information

Additional tables and figures. This material is available free of charge via the Internet at <http://pubs.acs.org>.

■ AUTHOR INFORMATION

Corresponding Author

*Phone: +86-571-88982341. Fax: +86-571-88982341. E-mail: shulin@zju.edu.cn (S.Z.) or wliu@zju.edu.cn (W.L.).

Funding

We acknowledge financial support from the National High-tech R&D Program of China (2013AA065202), the National Natural Science Foundation of China (Nos. 21277122 and 21107094), and the National Basic Research Program of China (2009CB421603).

Notes

The authors declare no competing financial interest.

■ REFERENCES

- (1) Sheehan, D. J.; Hitchcock, C. A.; Sibley, C. M. Current and emerging azole antifungal agents. *Clin. Microbiol. Rev.* **1999**, *12*, 40–79.
- (2) Goetz, A. K.; Ren, H. Z.; Schmid, J. E.; Blystone, C. R.; Thillainadarajah, I.; Best, D. S.; Nichos, H. P.; Strader, L. F.; Woff, D. C.; Narotsky, M. G.; Rochett, J. C.; Dix, D. J. Disruption of testosterone homeostasis as a mode of action for the reproductive toxicity of triazole fungicides in the male rat. *Toxicol. Sci.* **2007**, *95*, 227–239.
- (3) Fent, K.; Weston, A. A.; Caminada, D. Ecotoxicology of human pharmaceuticals. *Aquat. Toxicol.* **2006**, *76*, 122–159.
- (4) Crofton, K. M.; Boncek, V. M.; Reiter, L. W. Hyperactivity induced by triadimefon, a triazolefungicide. *Fundam. Appl. Toxicol.* **1988**, *10*, 459–465.
- (5) Wolf, D. C.; Allen, J. W.; George, M. H.; Hester, S. D.; Sun, G. B.; Moore, T.; Thai, S. F.; Delker, D.; Winkfield, E.; Leavitt, S.; Nelson, G.; Roop, B. C.; Jones, C.; Thibodeaux, J.; Nesnow, S. Toxicity profiles in rats treated with tumorigenic and nontumorigenic triazole conazole fungicides: propiconazole, triadimefon, and myclobutanil. *Toxicol. Pathol.* **2006**, *34*, 895–902.
- (6) Tully, D. B.; Bao, W.; Goetz, A. K.; Blystone, C. R.; Ren, H.; Schmid, J. E.; Strader, L. F.; Wood, C. R.; Best, D. S.; Narotsky, M. G.; Wolf, D. C.; Rockett, J. C.; Dix, D. J. Gene expression profiling in liver

and testis of rats to characterize the toxicity of triazolefungicides. *Toxicol. Appl. Pharmacol.* **2006**, *215*, 260–273.

- (7) Zhang, G. W.; Wang, L.; Pan, J. H. Probing the binding of the flavonoid diosmetin to human serum albumin by multispectroscopic techniques. *J. Agric. Food Chem.* **2012**, *60*, 2721–2729.

- (8) Wang, C.; Li, Y. Study on the binding of propiconazole to protein by molecular modeling and a multispectroscopic method. *J. Agric. Food Chem.* **2011**, *59*, 8507–8512.

- (9) Peters, T. *All about Albumin: Biochemistry, Genetics, And Medical Applications*; Academic Press: San Diego, CA, 1996.

- (10) Zhou, X. M.; Lv, W. J.; Su, L.; Shan, Z. J.; Chen, X. G. Binding of phthalate plasticizers to human serum albumin in vitro: a multispectroscopic approach and molecular modeling. *J. Agric. Food Chem.* **2012**, *60*, 1135–1145.

- (11) Gokara, M.; Sudhamalla, B.; Amooru, D. G.; Subramanyam, R. Molecular interaction studies of trimethoxy flavone with human serum albumin. *PLoS One* **2012**, *5*, e8834.

- (12) Abou-Zied, O. K.; Al-Shihi, O. I. K. Characterization of subdomain IIA binding site of human serum albumin in its native, unfolded, and refolded states using small molecular probes. *J. Am. Chem. Soc.* **2008**, *130*, 10793–10801.

- (13) Xiang, G. H.; Tong, C. L.; Lin, H. Z. Nitroaniline isomers interaction with bovine serum albumin and toxicological implications. *J. Fluoresc.* **2007**, *17*, 512–521.

- (14) Pettipas, I.; Bhattacharya, A. A.; Twine, S.; East, M.; Curry, S. Crystal structure analysis of warfarin binding to human serum albumin. *J. Biol. Chem.* **2001**, *276*, 22804–22809.

- (15) Ding, F.; Diao, J. X.; Sun, Y.; Sun, Y. Bioevaluation of human serum albumin-hesperidin bioconjugate: insight into protein vector function and conformation. *J. Agric. Food Chem.* **2012**, *60*, 7218–7228.

- (16) Verdonk, M. L.; Cole, J. C.; Hartshorn, M. J.; Murray, C. W.; Taylor, R. D. Improved protein ligand docking using GOLD. *Proteins: Struct. Funct. Genet.* **2003**, *52*, 609–623.

- (17) Wang, Y. Q.; Wang, X. Y.; Wang, J.; Zhao, Y. M.; He, W. J.; Guo, Z. J. Noncovalent interactions between a trinuclear monofunctional platinum complex and human serum albumin. *Inorg. Chem.* **2011**, *50*, 12661–12668.

- (18) Ware, W. R. Oxygen quenching of fluorescence in solution: an experimental study of the diffusion process. *J. Phys. Chem.* **1962**, *66*, 455–458.

- (19) Lu, Y.; Feng, Q. Q.; Cui, F. L.; Xing, W. W.; Zhang, G. S.; Yao, X. J. Interaction of 30-azido-30-deamino daunorubicin with human serum albumin: investigation by fluorescence spectroscopy and molecular modeling methods. *Bioorg. Med. Chem. Lett.* **2010**, *20*, 6899–6904.

- (20) Eftink, M. R.; Ghiron, C. A. Fluorescence quenching studies with proteins. *Anal. Biochem.* **1981**, *144*, 199–227.

- (21) Lakowicz, J. R. *Principles of Fluorescence Spectroscopy*, 3rd ed.; Springer Science+Business Media: New York, 2006.

- (22) Lakowicz, J. R.; Weber, G. Quenching of fluorescence by oxygen: a probe for structural fluctuations in micromolecules. *Biochemistry* **1973**, *12*, 4161–4170.

- (23) Nemethy, G.; Scheraga, H. A. The structure of water and hydrophobic bonding in proteins. III. The thermodynamic properties of hydrophobic bonds in proteins. *J. Phys. Chem.* **1962**, *66*, 1773–1789.

- (24) Ross, P. D.; Subramanian, S. Thermodynamics of protein association reactions: forces contributing of stability. *Biochemistry* **1981**, *20*, 3096–3102.

- (25) Ross, P. D.; Rekharsky, M. V. Thermodynamics of hydrogen bond and hydrophobic interactions in cyclodextrin complexes. *Biophys. J.* **1996**, *71*, 2144–2154.

- (26) Pan, X. R.; Qin, P. F.; Liu, R. T.; Wang, J. Characterizing the interaction between tartrazine and two serum albumins by a hybrid spectroscopic approach. *J. Agric. Food Chem.* **2011**, *59*, 6650–6656.

- (27) Ma, C. Q.; Li, K. A.; Zhao, F. L.; Tong, S. Y. A study on the reaction mechanism between chrome-azurol S and bovine serum albumin. *Acta Chim. Sinica* **1999**, *57*, 389–395.

- (28) Sulkowska, A. Interaction of drugs with bovine and human serum albumin. *J. Mol. Struct.* **2002**, *614*, 227–232.
- (29) Deeb, O.; Rosales-Hernández, C.; Gómez-Castro, C.; Garduño-Juárez, R.; Correa-Basurto, J. Exploration of human serum albumin binding sites by docking and molecular dynamics flexible ligand-protein interactions. *Biopolymers* **2009**, *93*, 161–170.
- (30) He, X. M.; Carter, D. C. Atomic structure and chemistry of human serum albumin. *Nature* **1992**, *358*, 209–215.
- (31) Bolel, P.; Mahapatra, N.; Halder, M. Optical spectroscopic exploration of binding of cochineal red A with two homologous serum albumins. *J. Agric. Food Chem.* **2012**, *60*, 3727–3734.
- (32) Abou-Zied, O. K.; Al-Lawatia, N. Exploring the drug-binding site Sudlow I of human serum albumin: the role of water and Trp214 in molecular recognition and ligand binding. *ChemPhysChem* **2011**, *12*, 270–274.
- (33) Wang, Y. Q.; Tang, B. P.; Zhang, H. M.; Zhou, Q. H.; Zhang, G. C. Studies on the interaction between imidacloprid and human serum albumin: spectroscopic approach. *J. Photochem. Photobiol. B–Biol.* **2009**, *94*, 183–190.
- (34) Charbonneau, D. M.; Tajmir-Riahi, H. A. Study on the interaction of cationic lipids with bovine serum albumin. *J. Phys. Chem. B* **2010**, *114*, 1148–1155.
- (35) Greenfield, N. J. Using circular dichroism spectra to estimate protein secondary structure. *Nat. Protoc.* **2006**, *1*, 2876–2890.